© 2022 Hefei Institutes of Physical Science, Chinese Academy of Sciences and IOP Publishing Printed in China and the UK Plasma Science and Technology

Plasma Sci. Technol. **24** (2022) 124010 (11pp) https://doi.org/10.1088/2058-6272/aca4b5

Recent progress of the ECRH system and initial experimental results on the J-TEXT tokamak

Donghui XIA (夏冬辉)*, Xixuan CHEN (陈曦璇), Dengfeng XU (徐登峰), Jiangang FANG (方建港), Junli ZHANG (张俊利), Nengchao WANG (王能超), Zhoujun YANG (杨州军), Zhongyong CHEN (陈忠勇), Yonghua DING (丁永华), Wei ZHENG (郑玮), Shaoxiang MA (马少翔), Zhijiang WANG (王之江) and Yuan PAN (潘垣)

International Joint Research Laboratory of Magnetic Confinement Fusion and Plasma Physics, State Key Laboratory of Advanced Electromagnetic Engineering and Technology, School of Electrical and Electronic Engineering, Huazhong University of Science and Technology, Wuhan 430074, People's Republic of China

E-mail: xiadh@hust.edu.cn

Received 24 August 2022, revised 19 November 2022
Accepted for publication 21 November 2022
Published 19 December 2022

Abstract

In order to broaden the range of the plasma parameters and provide experimental conditions for physical research into high-performance plasma, the development of the electron cyclotron resonance heating (ECRH) system for the J-TEXT tokamak was initiated in 2017. For the first stage, the ECRH system operated successfully with one 105 GHz/500 kW/1 s gyrotron in 2019. More than 400 kW electron cyclotron (EC) wave power has been injected into the plasma successfully, raising the core electron temperature to 1.5 keV. In 2022, another 105 GHz/500 kW/1 s gyrotron completed commissioning tests which signifies that the ECRH system could generate an EC wave power of 1 MW in total. Under the support of the ECRH system, various physical experiments have been carried out on J-TEXT. The electron thermal transport in ECRH plasmas has been investigated. When ECRH is turned on, the electron thermal diffusivity significantly increases. The runaway current is elevated when a disruption occurs during ECRH heating. When the injected EC wave power is 400 kW, the conversion efficiency of runaway current increases from 35% to 75%. Fast electron behavior is observed in electron cyclotron current drive (ECCD) plasma by the fast electron bremsstrahlung diagnostic (FEB). The increase in the FEB intensity implies that ECCD could generate fast electrons. A successful startup with a 200 kW ECW is achieved. With the upgrade of the ECRH system, the J-TEXT operational range could be expanded and further relevant research could be conducted.

Keywords: ECRH, J-TEXT tokamak, electron thermal transport, runaway electron current, assisted start-up

(Some figures may appear in colour only in the online journal)

1. Introduction

As one of the most promising methods for plasma heating and current profile control, electron cyclotron resonance heating (ECRH) has been widely applied in recent nuclear fusion research (e.g., DIII-D, W7-X, ASDEX-U, EAST, HL-2A) [1–5], and will be developed for future fusion devices. Since 2017, the development of a second-harmonic ECRH system with X-mode injection for Joint-TEXT (J-TEXT) has been initiated. J-TEXT is a conventional iron core tokamak reconstructed from the Texas Experimental Tokamak Upgrade (TEXT-U).

* Author to whom any correspondence should be addressed.

As a long-term research project, the J-TEXT physical research aims to develop basic physics and control mechanisms of high-performance tokamak plasma confinement and stability in support of the effective operation of the ITER and the design of the future Chinese fusion engineering testing reactor (CFETR). This ECRH system is established in order to provide experimental conditions for J-TEXT research. There are some special auxiliary systems, e.g., massive gas injection (MGI), shattered pellet injection (SPI), resonant magnetic perturbation (RMP) and abundant diagnostic systems on J-TEXT, which could be used in combination with ECRH to conduct more advanced experiments. ECRH has been used to study thermal transport in plasmas [6–8] and for pre-ionization and startup assistance in tokamaks [9, 10]. ECCD is an effective tool for controlling the magnetohydrodynamic (MHD) modes at resonant surfaces, particularly the $m/n = 2/1$ neoclassical tearing mode, which will cause disruption [11–13]. In addition, ECCD can also be used to modify the current profile which can form a reversed magnetic shear [14, 15] and sawtooth control in the vicinity of a $q = 1$ surface [16]. The plasma operation with the ECRH system will assist physical research on plasma heating, current drive, fast electron-related physics, the control of magnetic islands and sawtooth, plasma disruption prevention or mitigation, plasma boundary physics, etc.

The J-TEXT ECRH system was firstly put into formal experiments in 2019. Up to now, more than 400 kW electron cyclotron (EC) wave power injection has been achieved, improving the core electron temperature from about 0.9 keV to about 1.5 keV [17, 18]. Simultaneously, physical experiments related to electron thermal transport and temperature fluctuations, elevation of runaway electron current, fast electron behavior in ECCD plasma, and ECRH assisted plasma startup have been carried out on J-TEXT with the support of the ECRH system. To improve the performance of the ECRH system, another GYCOM gyrotron of 105 GHz/500 kW/1 s has finished its commissioning tests successfully in 2022, making the ECRH system on J-TEXT capable of providing up to 1 MW of EC wave power. Figure 1 gives the layout diagram of the J-TEXT ECRH system and its main parameters are shown in table 1.

In this paper, the recent progress of the J-TEXT ECRH system and the related experimental results will be presented. In section 2, the detailed composition of the ECRH system is introduced. Section 3 shows the performance of the ECRH system in the commissioning phase. Section 4 describes experimental studies carried out on J-TEXT with the assistance of the ECRH system. Finally, a summary is given in section 5.

2. J-TEXT ECRH system

In the initial design phase of the system, it is crucial to decide the output parameters of the ECRH system. Considering that J-TEXT is generally operated at the toroidal field of 1.4–2.2 T, mostly around 1.8 T, this system is considered to work at the X2 mode and 105 GHz, which could realize effective heating in the resonant layers. To generate a high-power EC wave with the desired frequency, the gyrotron is the core component. In the J-TEXT ECRH system, there are two gyrotrons which are manufactured by GYCOM Ltd. Safe and stable operation of the gyrotrons requires the participation of several subsystems and devices. Besides, it is also crucial that the high-power EC wave is effectively transmitted and injected into the plasma, which is realized by the transmission line and the launcher. Figure 2 shows the composition diagram of the ECRH system. This section elaborates on the components mentioned above.

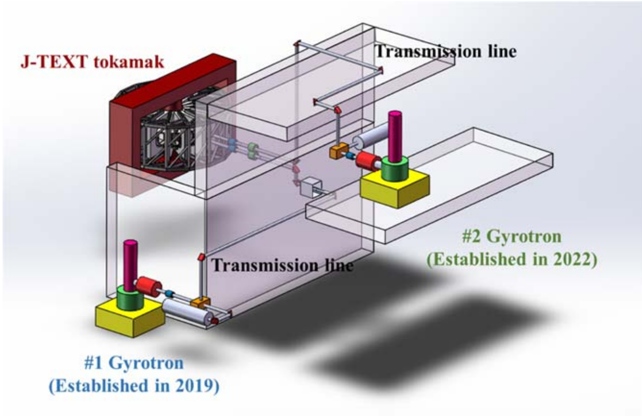

Figure 1. Layout of J-TEXT ECRH system [19]. Reproduced from [19]. CC BY 4.0.

Table 1. Main parameters of J-TEXT ECRH system.

ECRH parameters	Maximum or typical value (#1 gyrotron)	Maximum or typical value (#2 gyrotron)
Wave frequency	105 GHz	105 GHz
Output power	500 kW	500 kW
Pulse duration	1 s	1 s
TEM_{00} mode purity (after MOU)	97%	98%
Efficiency	45%	45%

2.1. Wave source and power supplies

As shown in figure 3, two GYCOM gyrotrons are already installed on the experimental site. Their output parameters are both 105 GHz/500 kW/1 s, thus in total the ECRH system could generate an EC wave of about 1 MW.

The stable operation of the ECRH system involves not only the gyrotron but also other auxiliary subsystems and devices. There are two main high-voltage power supplies, three auxiliary power supplies and some circuit units working together to meet the operation requirements.

The electrical parameters of the power supplies (PSs) are listed in table 2. The cathode power is the main source of the gyrotron beam current, therefore it must be capable of high voltage and large current output [20]. The anode power supply provides reverse voltage so that the beam current could be absorbed by the collector, it does not need large current output, the output voltage is around 30 kV [21].

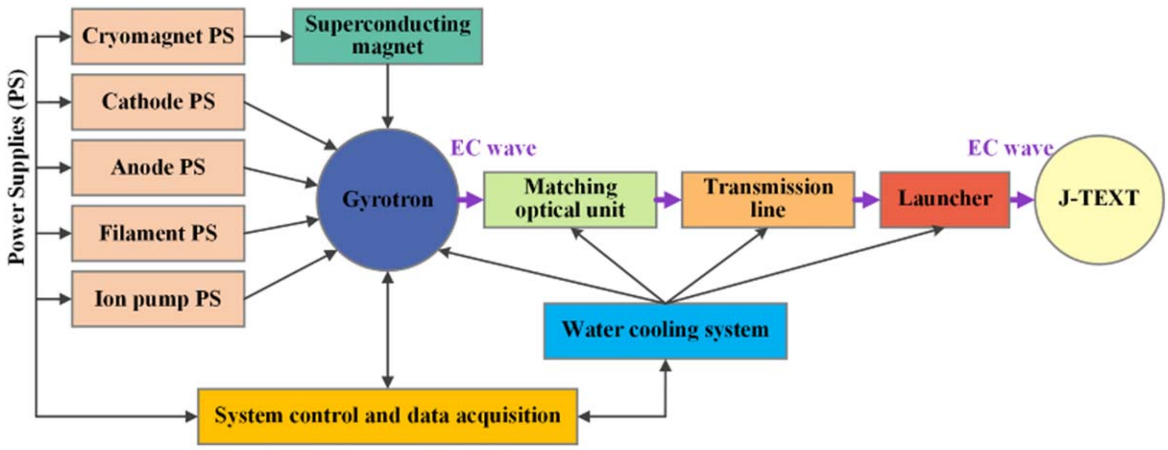

Figure 2. Composition diagram of J-TEXT ECRH system.

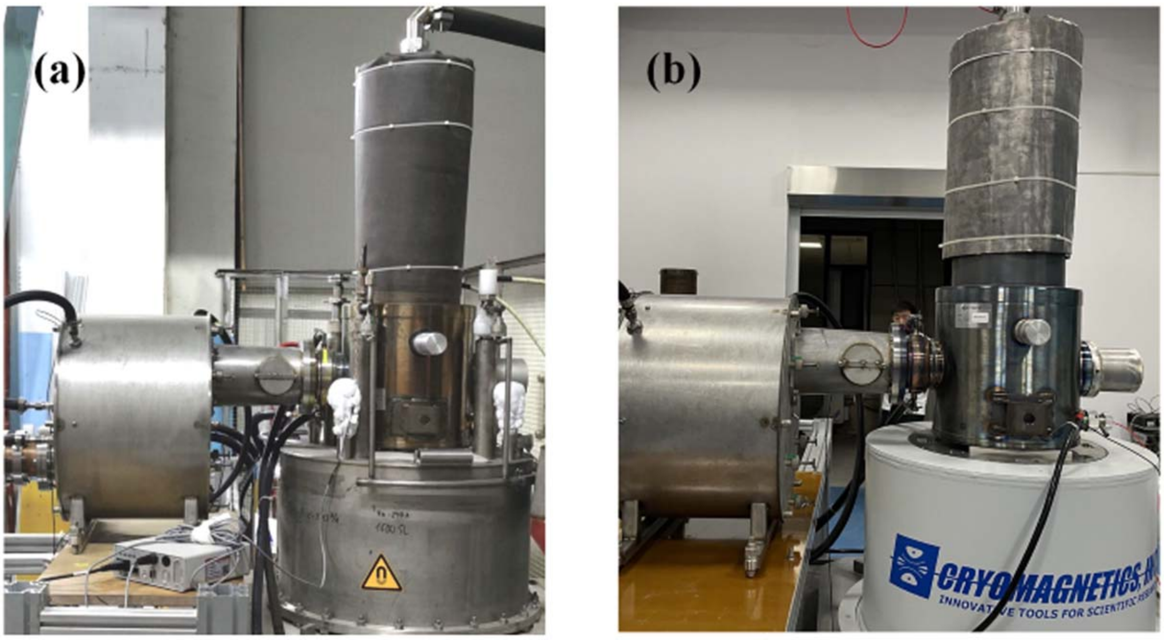

Figure 3. #1 gyrotron (a) and #2 gyrotron (b) of the 105 GHz ECRH system.

Furthermore, the anode power supply should also be capable of modulated output, so that the gyrotron could generate a modulated EC wave, which is very beneficial for physical experiments. At present, the anode power supply has a modulation frequency range of 1 Hz to 1 kHz. The duty cycle and modulation ratio could also be set flexibly.

2.2. Control system

The ECRH system requires a specialized control system to coordinate the operation of those subsystems and devices in the whole system. The control system designed for the J-TEXT ECRH system can realize time sequence trigger, protection [22], signal monitoring, communication, and data acquisition. By applying National Instruments CompactRIO devices and PXI devices in the control system hardware design, and realizing the software by LabVIEW, we have implemented a fully functional control system.

Table 2. Electrical parameters of power supplies for the gyrotron.

Power supply	Parameters (#1 gyrotron)	Parameters (#2 gyrotron)
Cathode power supply	−44 kV/25 A	−45 kV/24 A
Anode power supply	30 kV/150 mA	32 kV/200 mA
Magnet power supply	100 A	100 A
Ion pump power supply	5 kV/10 mA	5 kV/10 mA
Filament power supply	1500 VA	2500 VA

Figure 4 shows the diagram of the control system structure. Control personal computers (PCs) are installed in J-TEXT main control room. The control program is running on one control PC, experimenters can set parameters and check the status of subsystems on the control panel. CompactRIO devices are used for time sequence trigger, protection, signal monitoring, and communication, while PXI series devices are

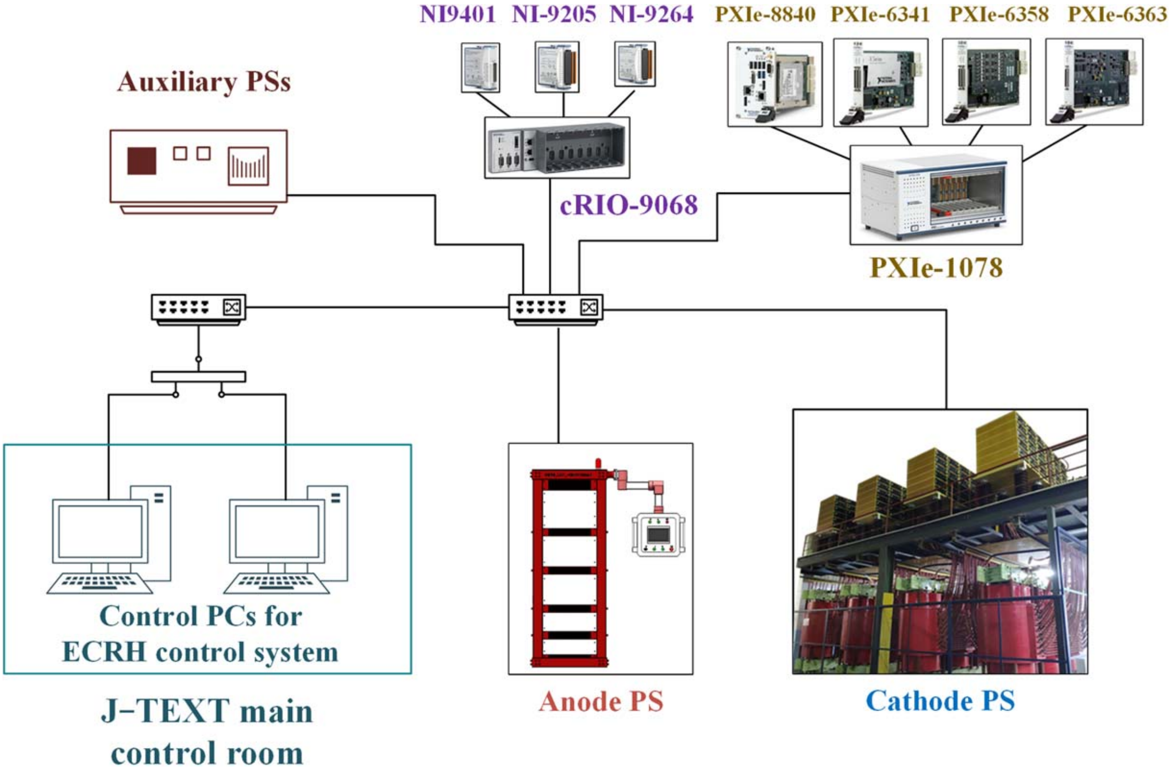

Figure 4. Diagram of ECRH control system structure.

used for data acquisition. Especially for fast protection of the control system, the action time could be limited within 2 μs. Until now, the control system has remained in a very stable condition and the failure rate is close to 0.05%.

2.3. Transmission line and launcher

The parts mentioned above can guarantee the basic normal operation of the ECRH system. Still, we need the transmission line and launcher to effectively transmit the high-power EC wave and inject it into the plasma.

The transmission line is based on corrugated waveguides with a diameter of 63.5 mm and is additionally composed of a switch, several miter bends, a directional coupler, a set of polarizers, a DC break and two bellows. Figure 5 shows some parts of this transmission line. The most concerned parameter of the transmission line is the transmission efficiency, which is closely linked with its transmission loss. The transmission loss is mainly caused at mitre bends. There is either flat mirror or polarizer on each bend. The amount of the transmission loss caused by those components is 7%–12%. Thus when 1 MW EC power is generated by the gyrotrons, more than 800 kW EC wave could be injected into the plasma.

To inject the high-power EC wave into the plasma, in 2019, a quasi-optical launcher was designed for the first ECRH system containing just one gyrotron [18]. In 2022, a dual-launcher has been designed for the present ECRH system. A drawing of the dual-launcher is shown in figure 6. This design is based on quasi-optical approximation and Gaussian optics, aiming to obtain an optimized localized power deposition in the center of the plasma. Considering the limitation of the port resource on the J-TEXT tokamak, for the dual-launcher, the toroidal injection angle can vary from $-10°$ to $+15°$, while the poloidal injection angle can vary from $-15°$ to $+15°$. As for the launcher focusing mirror, its focal length is chosen as 320 mm and hence the beam radius in the plasma center could reach a minimum value of 19.14 mm.

3. Performance of J-TEXT ECRH system

Before the ECRH system was put into experiments, some tests were carried out to confirm the performance of the system. In the commissioning tests, the optimal status of the gyrotron has been obtained and the alignment of the transmission line has been completed. After that, high-power commissioning tests have been carried out utilizing a dummy load to absorb the high-power microwave. Finally, the performance of the ECRH system has been tested by injecting the microwave into the plasma.

3.1. Beam patterns

Before the EC waves are injected into the plasma, it is necessary to carry out commissioning tests to guarantee the stable operation of the system. After the installation of the gyrotron, the matching optical unit (MOU) was connected to the output window to convert the output wave to Gaussian-like distribution. On this basis, the operating characteristics of the gyrotron could be explored to obtain the optimal status. Finally, the transmission line has been installed to transmit the EC wave from the wave source to the tokamak. The alignment of the transmission line is

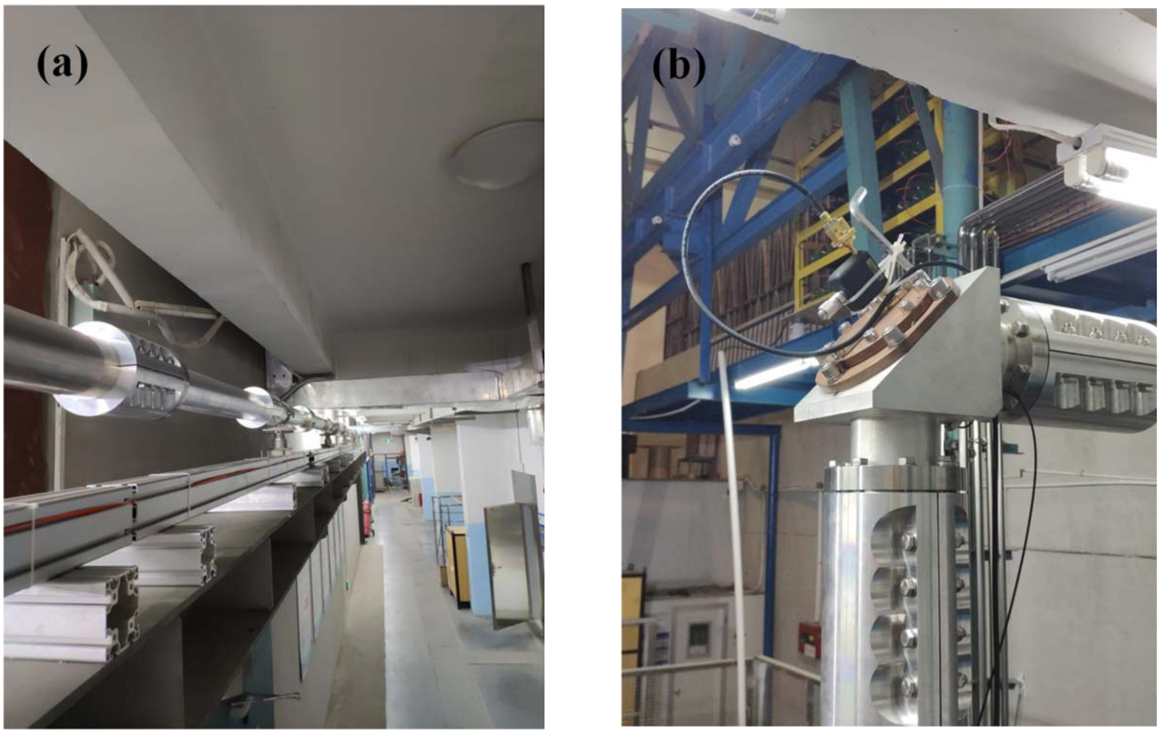

Figure 5. Part of the transmission line in J-TEXT ECRH system.

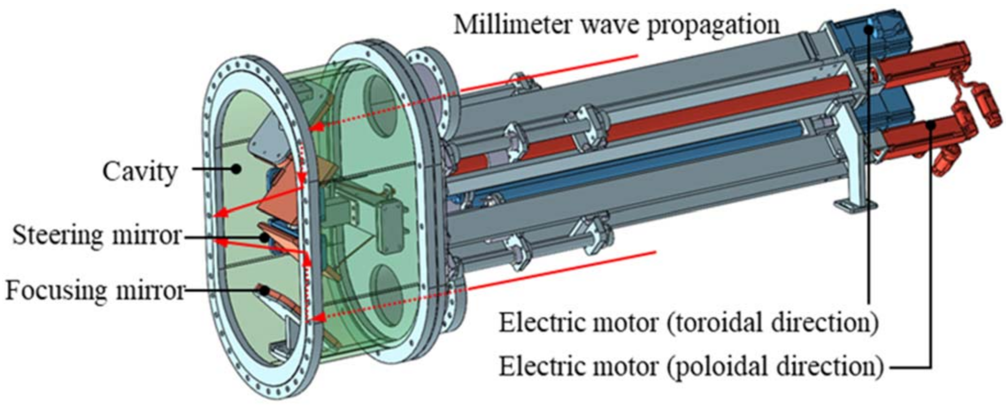

Figure 6. Drawing of the dual-launcher for J-TEXT ECRH system.

of great significance in transmitting the EC wave effectively and avoiding arc in it.

Figures 7(a) and (b) show the beam patterns generated by #1 gyrotron at the output of MOU and the end of the transmission line. Since the installation of the transmission line for #2 gyrotron has not yet been accomplished, its beam pattern was only measured at the output of MOU, which is given in figure 7(c). Each beam pattern has a Gaussian distribution and its center coincides with the center of output, which indicates that a good alignment has been obtained.

3.2. Power measurement and modulation

In the high-power tests of the ECRH system, the EC wave power has been injected into the water-cooled dummy load by switching the switch in the transmission line. There are generally two ways to measure the wave power in the ECRH system, which are the calorimetric method and the directional coupler method. The calorimetric method utilizes the thermal effect of the microwave on water, the average power of the microwave could be calculated by measuring temperature rise of the cooling water flowing in the dummy load or the MOU [23]. The directional coupler method couples a little part of the microwave power, which is measured by matched detectors, enabling real-time power monitoring of the ECRH system. Multi-hole directional couplers have been designed and fabricated for the J-TEXT ECRH system, and their reliability and sensitivity have been verified by the high-power test [24].

In the J-TEXT ECRH system, these two methods are combined to measure the power of EC waves, as shown in figure 8. The calorimetric method is used to measure the average EC power of one pulse, whereas the directional coupler method is used to measure the real-time power.

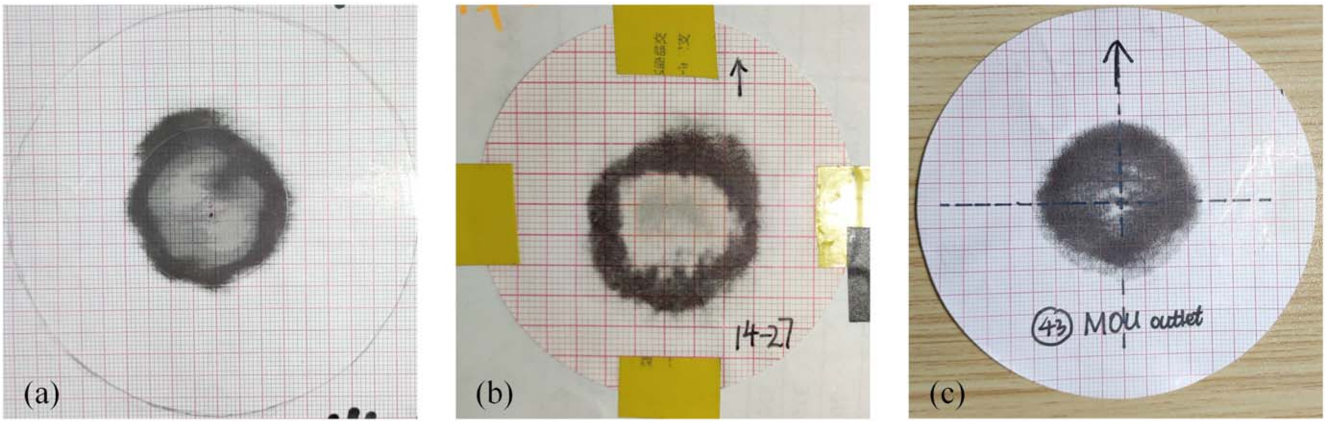

Figure 7. Beam patterns generated by #1 gyrotron at the output of MOU (a), at the end of the transmission line (b), and by #2 gyrotron at the output of MOU (c).

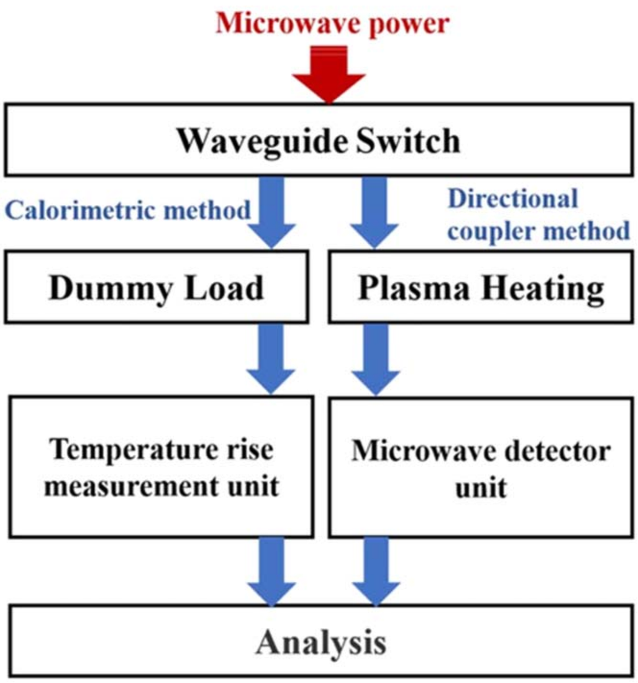

Figure 8. Schematic of EC wave power measurement in the J-TEXT ECRH system. Reproduced from [24]. © 2022 Hefei Institutes of Physical Science, Chinese Academy of Sciences and IOP Publishing. All rights reserved.

The output power of the gyrotron is affected by many parameters, such as the magnet field, the filament power, the cathode voltage and anode voltage. In the high-power operation, the EC wave power is normally controlled by adjusting the anode voltage. Figure 9 shows the temperature rise signal of one pulse for the two gyrotrons. In figure 9(a), the cathode and anode voltage were set to −40 kV and 24.5 kV for #1 gyrotron, and the pulse width were set to 500 ms. Before the high-power operation, the calibration was done to obtain the coefficient between the temperature signal integration and the EC wave power, which would be influenced by environmental factors such as temperature and flow rate [23]. Based on this, the average power of EC wave was calculated using the temperature rise signal, which was about 417 kW [25]. For the shot in figure 9(b), the cathode and anode voltages were −42 kV and 24 kV for #2 gyrotron, the pulse width was 400 ms, and an EC wave power of about 468 kW was obtained.

Due to the requirements of the experiments, sometimes the EC wave power injected into the plasma needs to be modulated, which could be achieved by the modulation of the anode voltage. Tests about the power modulation of the EC wave have been carried out based on #1 gyrotron. Figure 10 shows a typical waveform of the power modulation. In this shot, the cathode voltage was about −40 kV, the anode voltage was about 16.5 kV and was switched on and off at a frequency of 100 Hz. The radio frequency signal was detected utilizing the directional coupler method, which indicates that the output power of the gyrotron changed rapidly with the anode voltage and was modulated successfully.

3.3. Plasma heating with the EC wave

After the commissioning tests and high-power tests were finished, in May 2019 the EC wave was injected to heat the plasma for the first time on J-TEXT in order to test the performance of the ECRH system. Figure 11 shows a typical shot of EC wave injection. In this shot, about 350 kW EC wave power has been injected into the plasma perpendicularly [18]. The electron density and plasma current were about $3 \times 10^{19}\ \mathrm{m}^{-3}$ and 140 kA respectively. After the EC wave was injected, a large increase in the electron temperature measured by the x-ray imaging crystal spectrometer was observed and the soft x-ray signal raised to around 0.6 a.u. from 0.2 a.u. The soft x-ray profile of this shot is shown in figure 12, demonstrating that well localized heating effect on J-TEXT has been achieved with ECRH injection.

4. ECRH-related experiments on J-TEXT

EC waves have been proven to be a useful tool for current drive, controlling of MHD instabilities especially $m/n = 2/1$ NTM, thermal transport studies and assisted startup. The main tasks assigned to the J-TEXT ECRH system are plasma heating, plasma disruption, assisted startup, MHD stability control and

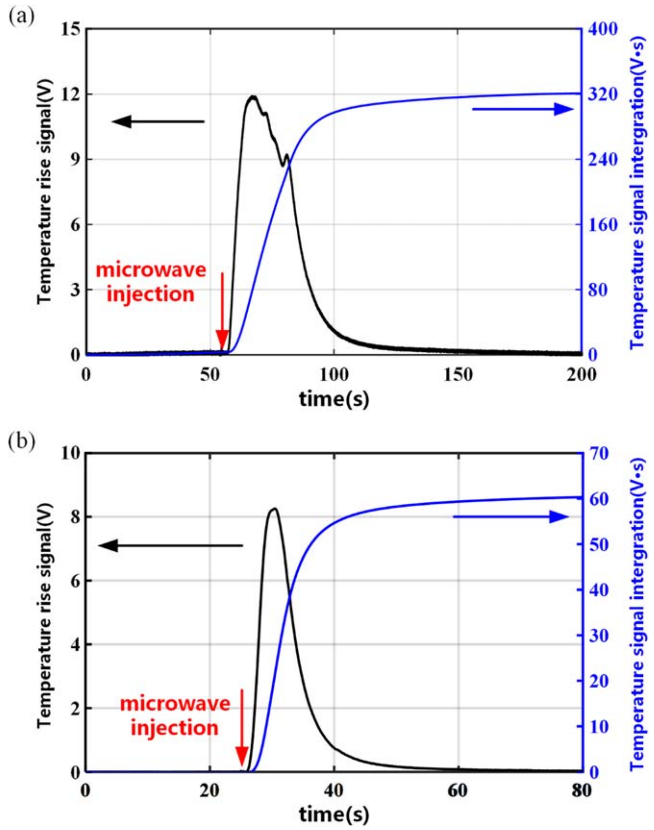

Figure 9. Temperature rise signal and its integration of gyrotron operation pulses. 417 kW, 500 ms operation pulse for #1 gyrotron (a). Reproduced from [25]. 468 kW, 400 ms operation pulse for #2 gyrotron (b).

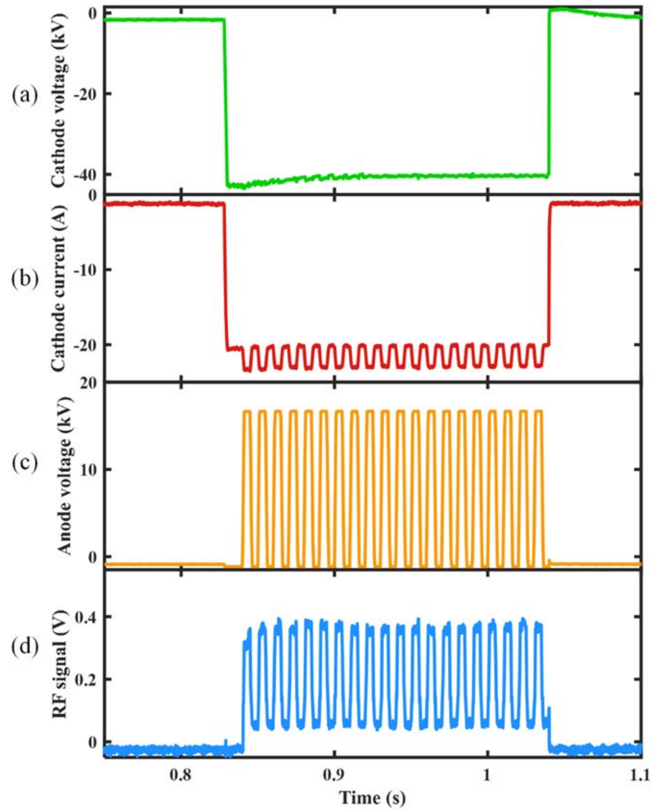

Figure 10. Waveform of the power modulation.

noninductive current drive. The ECRH system works at the frequency of 105 GHz, thus when the toroidal field B_t of the J-TEXT tokamak is 1.875 T, the EC wave power could deposit at the center of the plasma. The electron cyclotron emission (ECE) diagnostic on J-TEXT has 24 channels and covers a wide frequency range of 80−125 GHz. The ECE diagnostic can provide almost the whole electron temperature profile with highly efficient relative calibration. This is also an advantage of choosing the ECRH system working frequency at 105 GHz. In this section, we summarized the up-to-date ECRH related experimental studies on J-TEXT. The first dedicated experiments on the electron thermal transport and thermal fluctuations in ECRH plasma have been carried out [26], the elevation of runaway electron current by ECRH during disruption is presented [27], the fast electron behavior in ECCD plasma was studied by the fast electron bremsstrahlung (FEB) diagnostic [28], and ECRH assisted startup experiments were carried out on J-TEXT [29].

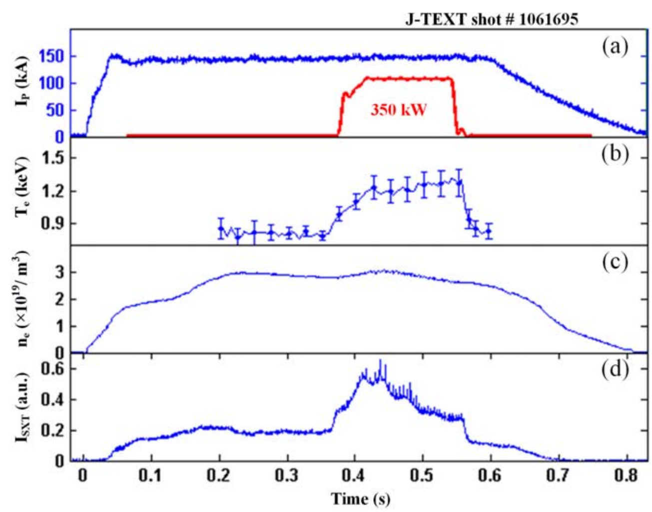

Figure 11. Typical shot of ECRH injection on J-TEXT. I_p is the plasma current (a), T_e is the electron temperature (b), n_e is the electron density (c), and I_{SXT} is the soft x-ray signal (d).

4.1. Study of electron thermal transport and temperature fluctuations

Relevant experimental results on DIII-D implies that long-wavelength electron temperature fluctuations play a vital role in affecting electron thermal transport [30, 31]. Furthermore, it was concluded that the high-k density fluctuation level could also influence the electron thermal transport [32]. Recently, the first specialized experiments have been conducted on J-TEXT to investigate electron thermal transport and temperature fluctuations in EC wave heated plasma. The change in temperature fluctuations is presented in figure 13(c). The broadband fluctuations width in electron

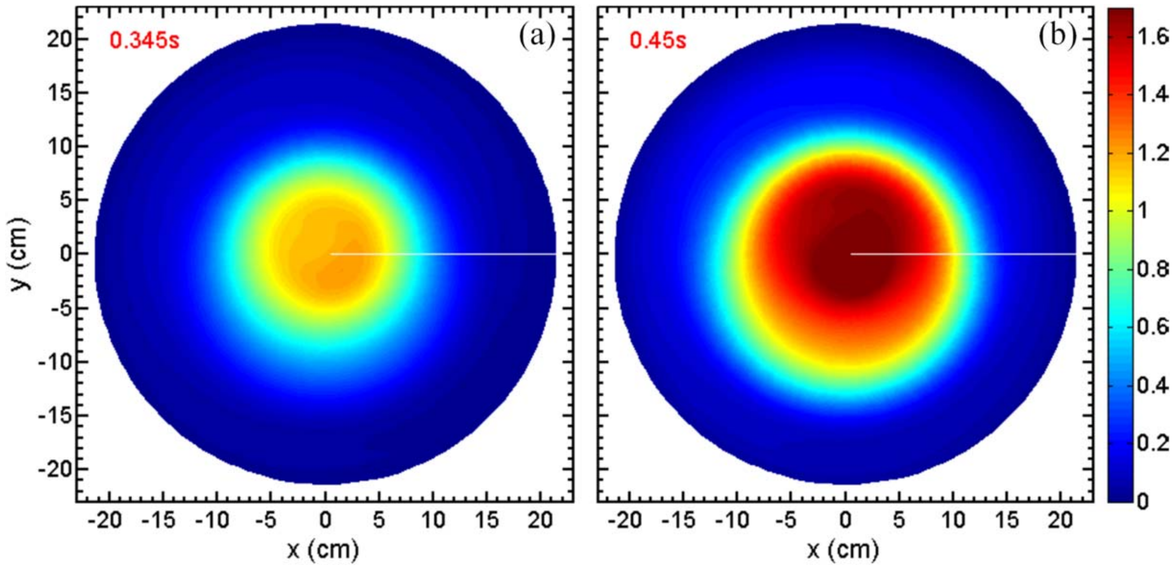

Figure 12. Soft x-ray profile before (a) and after (b) ECRH injection. © 2020 IEEE. Reprinted, with permission, from [18].

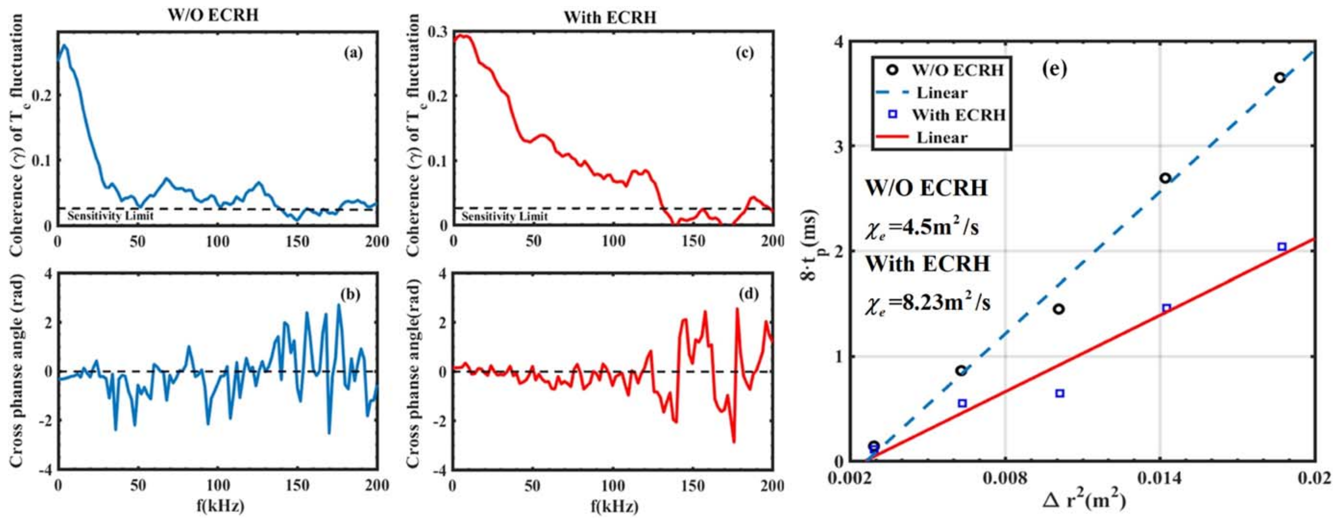

Figure 13. (a) and (c) Coherence (γ) without ECRH and with ECRH, respectively. (b) and (d) the cross-phase spectrum of two correlation electron cyclotron emission (CECE) diagnostic signals at $r/a = 0.7$ without ECRH and with ECRH, respectively. The red solid line and blue dashed line represent the fitting results with and without ECRH, respectively. Reproduced courtesy of IAEA. Figure from [26]. Copyright 2021 IAEA.

temperature increases from 50 kHz to 150 kHz in the spectrum. A sawtooth collapse might generate the heat pulse. Figure 13(e) shows that the different heat pulse peak moments ($8t_p$) and different relative positions Δr^2 have a linear relation. The electron thermal diffusivities are represented by the inverse slope of the fits in figure 13(e). The electron thermal diffusivities and temperature fluctuations are calculated before and after ECRH is applied, which is similar to previous findings in other devices [31]. The electron thermal transport diffusivities and temperature fluctuations have a simultaneous increase which could explain that long-wavelength electron temperature fluctuations do have an obvious effect on electron thermal transport [26].

4.2. Elevation of runaway electron current by ECRH during disruption

The high-energy runaway electrons (REs) during disruption will threaten the safe operation of a fusion reactor [33, 34]. It is of great importance to study the mechanisms of suppression of REs. Runaway electrons can be suppressed by ECRH in current flat-top phase. If a disruption occurs during ECRH, the runaway electron production may increase due to the generation of a suprathermal population. Recently, runaway current during disruption has been elevated by ECRH on the J-TEXT tokamak. The runaway current generation with/without ECRH is shown in figure 14. The massive gas injection (MGI) is used to trigger the disruption to generate a

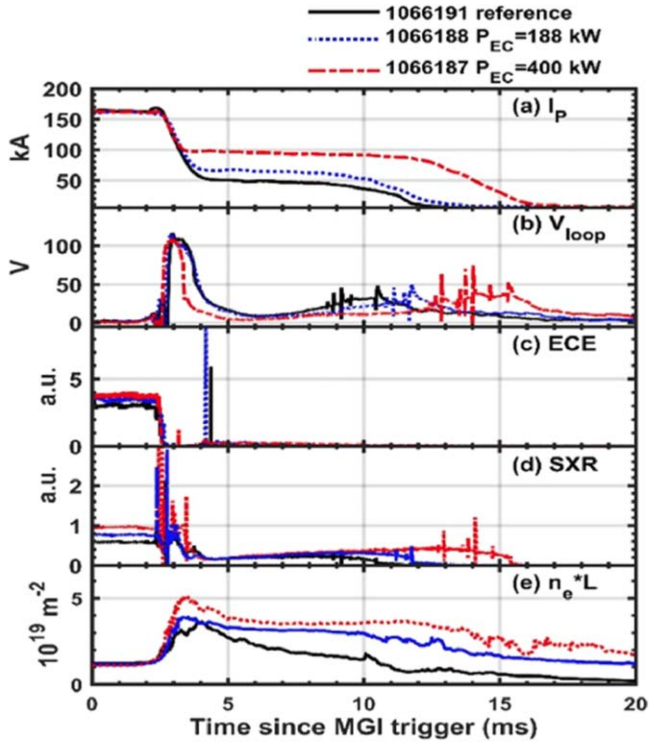

Figure 14. Time evolution of runaway current discharge with or without ECRH [27]. (a) Plasma current, (b) loop voltage, (c) ECE signals at $r = 1$ cm, (d) SXR radiation, (e) line-integrated density at plasma core. The reference time $t = 0$ ms was selected as the MGI trigger time. Reproduced from [27].

post-disruption runaway current plateau. The runaway current during disruption is elevated by ECRH. The ratio of runaway current and plasma current is up to 75% when 400 kW ECRH is applied. The slowing down time of the suprathermal electrons becomes large during disruption and acts as the hot tail, which leads to the elevation of runaway current [27].

4.3. Study of fast electron behavior in ECCD plasma

When the resonant condition is satisfied, the EC wave can interact with the plasma to generate fast electrons [35]. The FEB diagnostic is an efficient tool for investigating ECCD plasma physics. Recently, fast electron behavior has been observed in J-TEXT ECCD experiments [28] by the FEB diagnostic which has nine chords. Figure 15 shows a typical ECCD discharge with a number of fast electrons. With the EC wave injection at 250 ms, the line integrated intensity signal from the central chord of FEB I_{FEB} begins to rise (figure 15(c)). The 80.5 GHz ECE signal was measured at +31.96 cm, which is outside the plasma. The amplitude of this ECE signal is dominated by the relativistically down-shifted emission of fast electrons. So in figure 15(e), the ECE signal at +31.96 cm can be employed to diagnose the population of fast electrons [36]. In the spectrum of FEB, as shown in figure 15(h), I_{FEB} increases significantly at all energies after ECCD is applied. The maximum energy of photons increases from 150 keV to 250 keV. In the electron velocity distribution, the fast electron tail is obvious, which

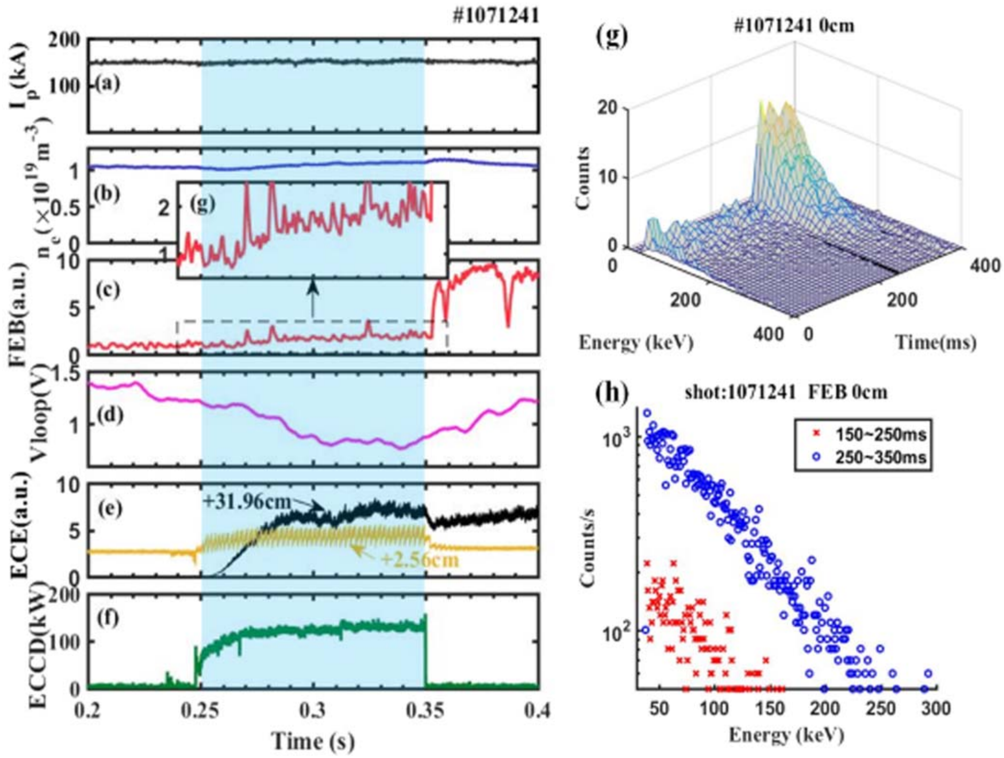

Figure 15. Temporal evolution of typical on-axis ECCD experiment which generated a large number of fast electrons. (a) Plasma current, (b) central line averaged electron density, (c) FEB signal at the plasma core, (d) loop voltage, (e) ECE signals at +2.56 cm and +31.96 cm, (f) ECCD power, (g) intensity of different energies with time, (h) energy spectrum before and during ECCD. Reproduced from [28].

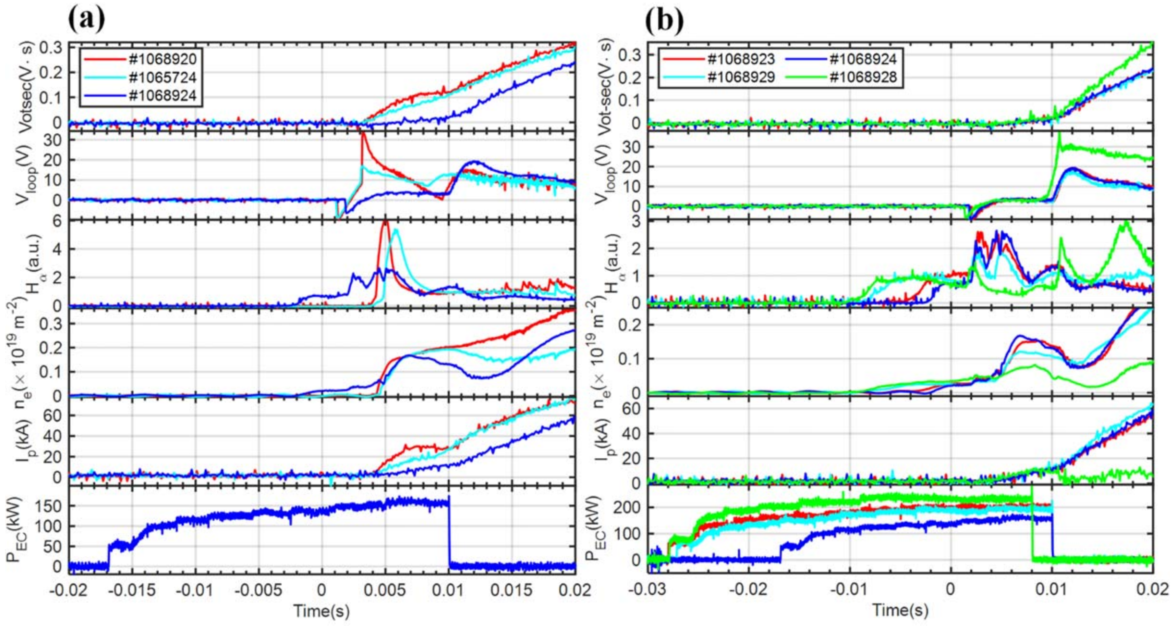

Figure 16. Evolutions of different signals (a) when discharging with ionization capacitor of 1600 V (red), 800 V (cyan) and 1 V (blue). The last one is assisted with 300 kW ECH power while the two others are purely Ohmic heating. (b) Different ECH pulse-width. Reproduced from [29]. CC BY 4.0.

indicates that fast electrons are generated when ECCD is applied.

4.4. ECRH assisted startup

Plasma can be formed by toroidal electric field acceleration in tokamaks. But the high toroidal electric field will cause quenching of superconducting coils, for example, ITER. ECRH pre-ionization makes low loop voltage startup possible. Recently, ECRH-assisted startup experiments have been conducted on J-TEXT, aiming to summarize the minimum experimental requirements and develop a better physical comprehension for the breakdown process [29].

Traditional Ohmic heating startup will cause a high breakdown voltage of about 34 V on J-TEXT. An extremely low breakdown voltage of 3.7 V was achieved by injecting 300 kW ECRH power into a vacuum vessel with a poloidal injection angle of 3°, as shown in figure 16(a). Further research reveals that ECRH pulse-width also has a significant effect on startup. Adjusting ECRH injection time, a successful startup with a low average ECRH power of 200 kW was achieved, as shown in figure 16(b). It suggests that injected time affects the required ECRH power for the startup.

5. Summary

A 105 GHz ECRH system has been designed and developed for the J-TEXT tokamak to improve the core electron temperature and broaden the operation regime. The performance of the ECRH system was tested, which showed that a well-localized heating effect could be achieved on J-TEXT with ECRH injection. The ECRH system was firstly put into an experiment in the spring of 2019 with one 105 GHz/500 kW/1 s gyrotron. Up to now, the core electron temperature has been raised to 1.5 keV successfully with a 400 kW ECRH injection. A new 105 GHz/500 kW/1 s gyrotron has been commissioned successfully on site in 2022, which indicates that the ECRH system is capable of providing 1 MW EC wave power in the future.

Many physical experiments related to ECRH/ECCD have been carried out with the assistance of the first ECRH system on J-TEXT. The electron thermal diffusivities in the ECRH phase are improved compared to that in the OH phase. The elevation of runaway current during plasma disruptions by ECRH has been investigated. When 400 kW EC power is applied, the conversion efficiency of runaway current increases to 75%. The fast electron behavior is observed in ECCD plasma by FEB diagnostic. The fast electron tail in the electron velocity distribution and the increase of the FEB intensity signal indicates that ECCD could produce fast electrons. A successful startup with a 200 kW ECW was achieved. ECRH pulse-width has a significant effect on the required ECRH power for the startup.

Acknowledgments

This work was supported by the National Key Research and Development Program of China (Nos. 2017YFE0300200 and 2017YFE0300204), the Key Research and Development Program of Hubei Province (No. 2021BAA167) and National Natural Science Foundation of China (No. 51821005).

References

[1] Cengher M *et al* 2014 *IEEE Trans. Plasma Sci.* **42** 1964
[2] Kasparek W *et al* 2005 *Fusion Eng. Des.* **74** 243
[3] Wagner D *et al* 2016 *J. Infrared Millim. Terahertz Waves* **37** 45
[4] Wang X J *et al* 2015 *Fusion Eng. Des.* **96–97** 181
[5] Huang M *et al* 2012 *EPJ Web of Conferences* **32** 04012
[6] Kirov K K *et al* 2006 *Plasma Phys. Control. Fusion* **48** 245
[7] Shi Z B *et al* 2007 *Plasma Sci. Technol.* **9** 534
[8] Song S D *et al* 2012 *Nucl. Fusion* **52** 033006
[9] Stober J *et al* 2011 *Nucl. Fusion* **51** 083031
[10] Sinha J *et al* 2022 *Nucl. Fusion* **62** 066013
[11] Zohm H *et al* 1997 *Phys. Plasmas* **4** 3433
[12] La Haye R J *et al* 2002 *Phys. Plasmas* **9** 2051
[13] Sheikh U A *et al* 2018 *Nucl. Fusion* **58** 106026
[14] Alikaev V V *et al* 2000 *Plasma Phys. Rep.* **26** 177
[15] Razumova K A *et al* 2000 *Plasma Phys. Control. Fusion* **42** 973
[16] Chapman I T *et al* 2013 *Plasma Phys. Control. Fusion* **55** 065009
[17] Wang N C *et al* 2022 *Nucl. Fusion* **62** 042016
[18] Zhang J L *et al* 2020 *IEEE Trans. Plasma Sci.* **48** 1560
[19] Chen X X *et al* 2022 *Proc. of the 21st Joint Workshop on Electron Cyclotron Emission (ECE) and Electron Cyclotron Resonance Heating (ECRH) (20–24 June 2022) (Saint-Paul-lez-Durance, France: ITER)*
[20] Ma S X *et al* 2014 *IEEE Trans. Plasma Sci.* **42** 656
[21] Xia D H *et al* 2018 *Plasma Sci. Technol.* **20** 014018
[22] Wang Z J *et al* 2021 *IEEE Trans. Plasma Sci.* **49** 258
[23] Wang H *et al* 2015 *EC18 18th Joint Workshop on Electron Cyclotron Emission and Electron Cyclotron Resonance Heating* 87 (Les Ulis: EDP Sciences) 02021
[24] Weng W T *et al* 2022 *Plasma Sci. Technol.* **24** 065602
[25] Xiong S Q *et al* 2022 *Plasma Sci. Technol.* **24** 105601
[26] Yang Z J *et al* 2021 *Nucl. Fusion* **61** 086005
[27] Bai W *et al* 2021 *Plasma Phys. Control. Fusion* **63** 115014
[28] Zhang X B *et al* 2022 *Plasma Sci. Technol.* **24** 064007
[29] Zhang J L *et al* 2022 *Proc. of the 21st Joint Workshop on Electron Cyclotron Emission (ECE) and Electron Cyclotron Resonance Heating (ECRH) (20–24 June 2022) (Saint-Paul-lez-Durance, France: ITER)*
[30] White A E *et al* 2010 *Phys. Plasmas* **17** 020701
[31] Schmitz L *et al* 2012 *Nucl. Fusion* **52** 023003
[32] Wang G *et al* 2011 *Phys. Plasmas* **18** 082504
[33] Hender T C *et al* 2007 *Nucl. Fusion* **47** S128
[34] Reux C *et al* 2015 *Nucl. Fusion* **55** 093013
[35] Turnbull A D *et al* 1995 *Phys. Rev. Lett.* **74** 718
[36] Fidone I and TFR Group 1981 *Phys. Rev.* A **24** 2861